

Localized N, Λ, Σ , and Ξ Single-Particle Potentials in Finite Nuclei Calculated with SU_6 Quark-Model Baryon-Baryon Interactions

M. Kohno¹ and Y. Fujiwara²

¹*Physics Division, Kyushu Dental College,
Kitakyushu 803-8580, Japan*

²*Department of Physics,
Kyoto University, Kyoto 606-8502, Japan*

Localized single-particle potentials for all octet baryons, N , Λ , Σ , and Ξ , in finite nuclei, ^{12}C , ^{16}O , ^{28}Si , ^{40}Ca , ^{56}Fe , and ^{90}Zr , are calculated using the quark-model baryon-baryon interactions. G -matrices evaluated in symmetric nuclear matter in the lowest order Brueckner theory are applied to finite nuclei in local density approximation. Non-local potentials are localized by a zero-momentum Wigner transformation. Empirical single-particle properties of the nucleon and the Λ hyperon in nuclear medium have been known to be explained semi-quantitatively in the LOBT framework. Attention is focused in the present consideration on predictions for the Σ and Ξ hyperons. The unified description for the octet baryon-baryon interactions by the SU_6 quark-model enables us to obtain less ambiguous extrapolation to the $S = -1$ and $S = -2$ sectors based on the knowledge in the NN sector than other potential models. The Σ mean field is shown to be weakly attractive at the surface, but turns to be repulsive inside, which is consistent with the experimental evidence. The Ξ hyperon s.p. potential is also attractive at the nuclear surface region, and inside fluctuates around zero. Hence Ξ hypernuclear bound states are unlikely. We also evaluate energy shifts of the Σ^- and Ξ^- atomic levels in ^{28}Si and ^{56}Fe , using the calculated s.p. potentials.

PACS numbers: 21.30.Fe, 21.65.-f, 21.80.+a

I. INTRODUCTION

One of the salient features of atomic nuclei is the success of the description of their properties by a single-particle (s.p.) picture. Although the nucleon-nucleon interaction is known to be strongly repulsive at the short range part, which was once conveniently described by a hard-core, the nucleon single-particle potential is well represented by a well-behaved local potential of the Woods-Saxon form. The theoretical base of understanding this circumstance in view of the singular two-body interaction was provided by the Brueckner theory in 1950's [1, 2, 3]. The progress of the density-dependent Hartree-Fock (DDHF) description of nuclear bulk properties followed in 1970's [4, 5], introducing some phenomenological adjustment for G -matrices in the Brueckner theory.

The mean field picture seems to hold also for hyperons in nuclei. For the Λ hyperon, the potential properties have been known from light to heavy nuclei from Λ formation and spectroscopy experiments [6]. Experimental studies of the Σ and Ξ hyperons in nuclear medium properties are now in progress. Because direct hyperon-nucleon scattering experiments are not readily available, the properties of the hyperon s.p. potentials are a valuable source of hyperon-nucleon interactions. This case, we have to resort to an effective interaction theory to relate s.p. properties of the hyperon embedded in nuclei with the character of hyperon-nucleon interactions.

In this paper we develop a method to obtain local potentials for octet baryons in finite nuclei with using full non-local G -matrix elements in nuclear matter, starting from the baryon-baryon bare interactions. The calcula-

tion of single-particle properties in nuclear matter can provide the basic information about the baryons in nuclear medium derived from the bare interaction. Nevertheless, it is instructive to explicitly calculate the s.p. potential in finite nuclei starting from two-body baryon-baryon interactions and compare them with the empirical ones. It is not even obvious whether the shape represented by the Woods-Saxon form which has been established both for the nucleon and the Λ hyperon mean fields is suitable for the Σ and the Ξ hyperons. The straightforward folding of the two-body effective interaction in momentum space provides a non-local potential in a nucleus. The non-locality also comes from the exchange character of the basic interaction. In order to make a comparison with empirical data, it is meaningful to define a local potential by some localization procedure. We employ in this paper a zero-momentum Wigner transformation method based on the WKB localization approximation [7].

It is necessary for a predictive discussion about hyperon s.p. properties in nuclei to use octet baryon-baryon bare interactions as reliable as possible. With little experimental information except for the ΛN interaction, the construction of the interactions in the strangeness $S = -1$ and $S = -2$ sectors is not simple, although some constraints are imposed by the flavor symmetry. The typical potential model has been developed in a one-boson-exchange potential (OBEP) picture by the Nijmegen group. The early parametrization with the hard-core in the 1970s [8, 9] has been successively revised by adjusting parameters in the soft core version [10, 11] and introducing new terms [13]. There are now a number of sets of parameters, reflecting ambiguities due to the lack

of experimental data. Although the description for the ΛN interaction seems to be under control, there are various uncertainties in the ΣN sector. For the Ξ hyperon, namely the strangeness $S = -2$ sector, the situation is no better.

Using the spin-flavor SU_6 quark-model, the Kyoto-Niigata group [14, 15, 16, 17, 18] have developed a unified description for the interactions between full octet baryons. In this model, the interaction is constructed as the Born kernel in the framework of the resonating group method for the three-quark clusters, the short range part of which is composed of the effective one-gluon exchange mechanism. The basic SU_6 symmetry provides a specific framework to the interactions between octet baryons and the Pauli principle respected on the quark level in addition brings about a characteristic structure to them. Incorporating effective meson exchange potentials between quarks, namely the scalar, pseudo-scalar, and vector mesons exchanges, the model is able to account the NN scattering data as accurately as other modern NN potential models.

Parameters of the SU_6 quark-model by the Kyoto-Niigata group are mostly fixed in the NN and ΛN sectors, and the uncertainties in the extension to the ΣN and ΞN channels are limited. In fact, the definite predictions such as the smallness of the ΛN spin-orbit interaction and the overall repulsive nature of the Σ -nucleus s.p. potential in nuclei have been supported by the experiments afterwards. Therefore it is interesting to examine the whole prediction of this potential for s.p. properties of all the octet baryons in nuclear medium. In particular, concrete predictions are presented for the Ξ hyperon. We use the most recent quark-model potential fss2 [17, 18] in this paper. The parameter set includes no adjustable parameter for the tuning afterward. The original interaction as a Born kernel has an inherent energy-dependence. Recently the method to eliminate the energy-dependence was developed [19]. We actually use this renormalized version of the fss2 potential.

We present, in Sec. II, basic expressions of the method to evaluate localized N , Λ , Σ , and Ξ s.p. potentials in a finite nucleus. We first discuss numerical results of these s.p. potentials in nuclear matter to represent basic characters of the G -matrices of the quark-model baryon-baryon interactions. Calculated results in finite nuclei, ^{12}C , ^{16}O , ^{28}Si , ^{40}Ca , ^{56}Fe , and ^{90}Zr , are shown in Sec. IV. The energy shift and the width of the Σ^- and Ξ^-

atomic levels in ^{28}Si and ^{56}Fe are studied in Sec. V on the basis of the s.p. potential obtained in Sec. IV. Summary is given in Sec. VI.

II. LOCALIZED SINGLE-PARTICLE POTENTIAL IN A FINITE NUCLEUS

We calculate a baryon single-particle potential in a finite nucleus which is defined by folding NN or YN G -matrix elements in nuclear matter with respect to nucleon occupied states through the local density approximation. It has been a traditional method for the microscopic study of bulk properties of nuclei to construct density-dependent two-body local interaction based on the G -matrices in nuclear matter and apply the effective interaction to mean field calculations for finite nuclei. Avoiding this procedure, we directly fold G -matrix elements to obtain non-local s.p. potentials and localize them. In the DDHF calculations, some phenomenological adjustments are introduced to reproduce the properties of the well-known nuclei. The purpose of the present paper is not to accomplish the reproduction of empirical values, but examine overall implications of the unified description of the baryon-baryon bare interaction by the quark model potential fss2 [18] for hyperon s.p. potentials in finite nuclei. In this section, we derive a basic expression for the s.p. potential, by introducing some approximations and a localized method by the zero-momentum Wigner transform.

A. direct term

First we consider the following direct term contribution. The wave function $\phi_{\ell_h j_h m_{j_h}}$ denotes the nucleon s.p. wave function of the nucleus with the orbital angular momentum ℓ_h and the total angular momentum j_h , and the dummy wave function of the baryon for which the potential is calculated is denoted by $\phi_{\ell_j m_j}$. The average over the z -component of the total angular momentum, $\frac{1}{\hat{j}} \sum_{m_j}$ with $\hat{j} \equiv 2j + 1$, means that we assume the spherical symmetry from the beginning. We do not write the isospin indices for simplicity in the following derivation, but recover them in the final expression.

$$\begin{aligned}
 I_D &\equiv \frac{1}{\hat{j}} \sum_{m_j} \sum_{hm_{j_h}} \iiint \int d\mathbf{r}_1 d\mathbf{r}_2 d\mathbf{r}'_1 d\mathbf{r}'_2 \phi_{\ell_j m_j}^*(\mathbf{r}'_1) \phi_{\ell_h j_h m_{j_h}}^*(\mathbf{r}'_2) G(\mathbf{r}'_1, \mathbf{r}'_2, \mathbf{r}_1, \mathbf{r}_2) \phi_{\ell_j m_j}(\mathbf{r}_1) \phi_{\ell_h j_h m_{j_h}}(\mathbf{r}_2) \\
 &= \sum_h \sum_{JMLL'S} \hat{j}_h \hat{S} \sqrt{\hat{L}\hat{L}'} \begin{Bmatrix} \ell & \ell_h & L \\ 1/2 & 1/2 & S \end{Bmatrix} \begin{Bmatrix} \ell & \ell_h & L' \\ j & j_h & J \end{Bmatrix} \iiint \int d\mathbf{r}_1 d\mathbf{r}_2 d\mathbf{r}'_1 d\mathbf{r}'_2 \\
 &\quad \times [[\phi_\ell^*(\mathbf{r}'_1) \times \phi_{\ell_h}^*(\mathbf{r}'_2)]^{L'} \times \chi_M^S] G(\mathbf{r}'_1, \mathbf{r}'_2, \mathbf{r}_1, \mathbf{r}_2) [[\phi_\ell(\mathbf{r}_1) \times \phi_{\ell_h}(\mathbf{r}_2)]^L \times \chi_M^S]. \tag{1}
 \end{aligned}$$

The effective baryon-baryon interaction $G(\mathbf{r}'_1, \mathbf{r}'_2, \mathbf{r}_1, \mathbf{r}_2)$ in a coordinate space is supposed to be related to the G -matrix in momentum space $G(\mathbf{k}', \mathbf{k}; K, \omega)$ by

$$G(\mathbf{r}'_1, \mathbf{r}'_2, \mathbf{r}_1, \mathbf{r}_2) = \frac{(2\pi)^3}{(2\pi)^{12}} \iiint d\mathbf{k}_1 d\mathbf{k}_2 d\mathbf{k}'_1 d\mathbf{k}'_2 \delta(\mathbf{K} - \mathbf{K}') e^{i(\mathbf{k}'_1 \cdot \mathbf{r}'_1 + \mathbf{k}'_2 \cdot \mathbf{r}'_2 - \mathbf{k}_1 \cdot \mathbf{r}_1 - \mathbf{k}_2 \cdot \mathbf{r}_2)} G(\mathbf{k}', \mathbf{k}; K, \omega), \quad (2)$$

Here each momentum has the following relation: $\mathbf{k}_1 = \frac{m_1}{m_1+m_2} \mathbf{K} + \mathbf{k}$, $\mathbf{k}_2 = \frac{m_2}{m_1+m_2} \mathbf{K} - \mathbf{k}$, $\mathbf{k}'_1 = \frac{m_1}{m_1+m_2} \mathbf{K}' + \mathbf{k}'$, $\mathbf{k}'_2 = \frac{m_2}{m_1+m_2} \mathbf{K}' - \mathbf{k}'$. The mass of the baryon for which the s.p. potential is evaluated is denoted by m_1 and the mass of the nucleon in the target nucleus by m_2 . The G -matrix is evaluated in symmetric nuclear matter by solving the baryon-channel coupling Bethe-Goldstone equations

$$G_{\alpha, \alpha'}(\mathbf{k}', \mathbf{k}; K, \omega) = V_{\alpha, \alpha'}(\mathbf{k}', \mathbf{k}; \mathbf{K}) + \frac{1}{(2\pi)^3} \sum_{\beta} \int d\mathbf{q} V_{\alpha, \beta}(\mathbf{k}', \mathbf{q}; \mathbf{K}) \frac{Q_{\beta}(q, K)}{\omega - E_b(k_1) - E_N(k_2)} G_{\beta, \alpha'}(\mathbf{q}, \mathbf{k}; K, \omega), \quad (3)$$

with the suffix specifying the pair of a baryon b and a nucleon N by β . The Pauli exclusion operator Q_{β} is treated in the standard angle-average approximation. The explicit expression may be found in ref. [20]. $E_a(k)$ is a s.p. energy of the baryon a in nuclear matter. We employ the continuous choice for the energy denominator in Eq. (3). That is, $E_a(k) = m_a + \frac{\hbar^2}{2m_a} k^2 + U_a(k)$ is defined self-consistently by the following definition of the s.p. potential U_a .

$$U_a(k) = \int d\mathbf{k}' G_{\alpha, \alpha}(\mathbf{q}, \mathbf{q}; \mathbf{k} + \mathbf{k}', \omega), \quad (4)$$

where $\mathbf{q} = \frac{1}{2}(\mathbf{k} - \mathbf{k}')$ and $\omega = E_{N,Y}(k) + E_N(k')$. The prescription for the starting energy ω in the local density approximation is explained in the next section.

The straightforward calculation of Eq. (1) needs much computational effort and is not fruitful to obtain a physical insight for baryon properties in nuclei by starting from the bare baryon-baryon interactions. We introduce two simplifying approximations. One is the spin-average in taking the sum of the matrix elements, which means that we take the average over the spin orientation:

$$\begin{aligned} & \frac{1}{\hat{S}} \sum_{M_S} \langle SM_S | G(\mathbf{k}', \mathbf{k}; K, \omega) | SM_S \rangle \\ &= \sum_{qJ_q} \frac{\hat{J}_q}{4\pi \hat{J}_q \hat{S}} G_{qq}^{J_q S}(k', k; K, \omega) P_q(\cos \widehat{\mathbf{k}\mathbf{k}'}), \end{aligned} \quad (5)$$

where the G -matrix is decomposed to partial waves and P_q stands for the Legendre polynomial with q specifying the orbital angular momentum. The other simplification is the following replacement.

$$\begin{aligned} & \iint d\mathbf{r}_1 d\mathbf{r}'_1 \phi_{\ell j m_j}^*(\mathbf{r}'_1) \phi_{\ell j m_j}(\mathbf{r}_1) \\ &= \iint d\mathbf{R}_1 d\mathbf{s}_1 \phi_{\ell j m_j}^*(\mathbf{R}_1 + \frac{1}{2}\mathbf{s}_1) \phi_{\ell j m_j}(\mathbf{R}_1 - \frac{1}{2}\mathbf{s}_1) \\ &\Rightarrow \int d\mathbf{R}_1 \phi_{\ell j m_j}^*(\mathbf{R}_1) \phi_{\ell j m_j}(\mathbf{R}_1) \int d\mathbf{s}_1. \end{aligned} \quad (6)$$

This corresponds to the zero-momentum Wigner transformation of the non-local potential. That is, we set

$p = 0$ for the Wigner transformation $U^W(\mathbf{R}, \mathbf{p})$ of the non-local potential $U(\mathbf{r}_1, \mathbf{r}_2)$.

$$U^W(\mathbf{R}, \mathbf{p}) = \int d\mathbf{s} e^{i\mathbf{p}\cdot\mathbf{s}} U(\mathbf{R} + \frac{1}{2}\mathbf{s}, \mathbf{R} - \frac{1}{2}\mathbf{s}). \quad (7)$$

Results shown in Sect. IV for nucleons and lambdas, for which we know what s.p. potentials are expected in G -matrix calculations with bare NN and ΛN interactions in various studies in literature, implies that the zero-momentum approximation works well. More direct confirmation of the reliability of this approximation will be presented elsewhere [21].

To evaluate Eq. (1) with the above simplification it is convenient to use the Fourier transform of the s.p. wave function $\phi_{\ell j m_j}$,

$$\begin{aligned} \tilde{\phi}_{\ell j m_j}(\mathbf{k}) &= \frac{1}{(2\pi)^3} \int d\mathbf{r} e^{-i\mathbf{k}\cdot\mathbf{r}} \phi(\mathbf{r}) \\ &= \frac{1}{(2\pi)^{3/2}} i^{2n-\ell} [Y_{\ell}(\hat{\mathbf{k}}) \times \chi_{1/2}]_{m_j}^j \frac{1}{k} \tilde{\phi}_{\ell j}(k), \end{aligned} \quad (8)$$

where n is a nodal quantum number and the Fourier transformation of the radial wave function is defined as

$$\frac{1}{k} \tilde{\phi}_{\ell j}(k) = (-i)^{2n} \sqrt{\frac{2}{\pi}} \int dr r j_{\ell}(kr) \phi_{\ell j}(r). \quad (9)$$

After carrying out some integrations and taking angular momentum recouplings, we obtain the final expression as follows.

$$\begin{aligned} I_D &= \frac{1}{4(4\pi)^2} \frac{1}{(2\pi)^3} \left(1 + \frac{m_2}{m_1}\right)^3 \sum_h \hat{J}_h \int dR_1 |\phi_{\ell}(R_1)|^2 \\ &\times \iint d\mathbf{k} d\mathbf{k}' j_0(|\mathbf{k}' - \mathbf{k}| R_1) \frac{1}{|\mathbf{Q}'_1|} \tilde{\phi}_{\ell_h}^*(|\mathbf{Q}'_1|) \\ &\times \frac{1}{|\mathbf{Q}_1|} \tilde{\phi}_{\ell_h}(|\mathbf{Q}_1|) P_{\ell_h}(\cos \widehat{\mathbf{Q}'\mathbf{Q}}) \\ &\times \sum_{qJ_q S} \hat{J}_q G_{qq}^{J_q S}(k, k') P_q(\cos \widehat{\mathbf{k}\mathbf{k}'}), \end{aligned} \quad (10)$$

where \mathbf{Q}_1 and \mathbf{Q}'_1 are defined by \mathbf{k} and \mathbf{k}' as

$$\mathbf{Q}_1 \equiv -\left(1 + \frac{m_2}{2m_1}\right)\mathbf{k} - \frac{m_2}{2m_1}\mathbf{k}', \quad (11)$$

$$\mathbf{Q}'_1 \equiv -\left(1 + \frac{m_2}{2m_1}\right)\mathbf{k}' - \frac{m_2}{2m_1}\mathbf{k}. \quad (12)$$

B. Exchange term

We also have to consider the exchange term contribution, which is familiar for the nucleon through the antisymmetrization of the wave function. For hyperons, such terms appear in association with the exchange character of the hyperon-nucleon interaction, which is realized by the strange meson exchange in the OBEP description. Denoting the space-exchange operator and the spin-exchange operator by P_r and P_σ , respectively, and specifying the even and odd components of the interac-

tion under the space-exchange, the matrix element of the YN interaction is written as

$$\begin{aligned} \langle YN|V|YN\rangle &= \langle YN|V_E\frac{1}{2}(1+P_r)+V_O\frac{1}{2}(1-P_r)|YN\rangle \\ &= \langle YN|\frac{1}{2}(V_E+V_O)|YN\rangle \\ &\quad -\langle YN|\frac{1}{2}(V_O-V_E)P_\sigma|NY\rangle, \end{aligned} \quad (13)$$

where the relation $P_\sigma P_r|NY\rangle = |YN\rangle$ is used. The first term was treated in the previous subsection as a direct term contribution, and the second term is considered in this subsection. The effective interactions in the direct and exchange contributions should be treated as such a combination of the even and odd parts in each spin and isospin channels, though the isospin dependence is disregarded in the above expression because the inclusion of it in the final expression is simple.

$$\begin{aligned} I_E &\equiv -\frac{1}{\hat{j}} \sum_{m_j} \sum_{hm_jh} \iiint \int d\mathbf{r}_1 d\mathbf{r}_2 d\mathbf{r}'_1 d\mathbf{r}'_2 \phi_{\ell_h j_h m_{j_h}}^*(\mathbf{r}'_1) \phi_{\ell_j m_j}^*(\mathbf{r}'_2) G(\mathbf{r}'_1, \mathbf{r}'_2, \mathbf{r}_1, \mathbf{r}_2) \phi_{\ell_j m_j}(\mathbf{r}_1) \phi_{\ell_h j_h m_{j_h}}(\mathbf{r}_2) \\ &= -\sum_h \sum_{JMLL'S} \hat{j}_h \hat{S} \sqrt{\hat{L}\hat{L}'} (-1)^{j+j_h-J} \begin{Bmatrix} \ell & \ell_h & L \\ 1/2 & 1/2 & S \end{Bmatrix} \begin{Bmatrix} \ell & \ell_h & L' \\ j & j_h & J \end{Bmatrix} \iiint \int d\mathbf{r}_1 d\mathbf{r}_2 d\mathbf{r}'_1 d\mathbf{r}'_2 \\ &\quad \times (-1)^{\ell_h+\ell+1+j_h+j+L'+S+J} [[\phi_{\ell_h}^*(\mathbf{r}'_1) \times \phi_{\ell}^*(\mathbf{r}'_2)]^{L'} \times \chi^S]_M^J G(\mathbf{r}'_1, \mathbf{r}'_2, \mathbf{r}_1, \mathbf{r}_2) [[\phi_{\ell}(\mathbf{r}_1) \times \phi_{\ell_h}(\mathbf{r}_2)]^L \times \chi^S]_M^J \end{aligned} \quad (14)$$

In this case we define \mathbf{R}_1 and \mathbf{s}_1 as

$$\mathbf{R}_1 = \frac{1}{2}(\mathbf{r}_1 + \mathbf{r}'_2), \quad \mathbf{s}_1 = \mathbf{r}'_2 - \mathbf{r}_1. \quad (15)$$

Introducing the same simplifying approximations as in the direct term, we obtain

$$\begin{aligned} I_E &= \frac{-1}{4(4\pi)^2} \frac{1}{(2\pi)^3} \left(1 + \frac{m_2}{m_1}\right)^3 \sum_h \hat{j}_h \int dR_1 |\phi_{\ell}(R_1)|^2 \\ &\quad \times \int \int d\mathbf{k} d\mathbf{k}' j_0(|\mathbf{k} + \mathbf{k}'|R_1) \frac{1}{|\mathbf{Q}'_2|} \tilde{\phi}_{\ell_h}^*(|\mathbf{Q}'_2|) \\ &\quad \times \frac{1}{|\mathbf{Q}_2|} \tilde{\phi}_{\ell_h}(|\mathbf{Q}_2|) P_{\ell_h}(\cos \widehat{\mathbf{Q}'_2 \mathbf{Q}_2}) \\ &\quad \times \sum_{qJ_q S} (-1)^{1+S} \hat{J}_q G_{qq}^{J_q S}(k, k') P_q(\cos \widehat{\mathbf{k} \mathbf{k}'}), \end{aligned} \quad (16)$$

where \mathbf{Q}_2 and \mathbf{Q}'_2 are defined by \mathbf{k} and \mathbf{k}' by

$$\mathbf{Q}_2 = -\left(1 + \frac{m_2}{2m_1}\right)\mathbf{k} + \frac{m_2}{2m_1}\mathbf{k}', \quad (17)$$

$$\mathbf{Q}'_2 = \left(1 + \frac{m_2}{2m_1}\right)\mathbf{k}' - \frac{m_2}{2m_1}\mathbf{k}. \quad (18)$$

These \mathbf{Q}_2 and \mathbf{Q}'_2 are obtained by changing the sign of \mathbf{k}' in \mathbf{Q}_1 and \mathbf{Q}'_1 of Eqs. (11) and (12). It is easy to see that the difference of the expressions of I_E and I_D is only the factor $(-1)^{S+q}$. Thus, recovering the isospin degrees of freedom, we obtain

$$\begin{aligned} I_D + I_E &= \frac{1}{4(4\pi)^2} \sum_{hS} \int dR_1 |\phi_{\ell}(R_1)|^2 \hat{j}_h \left(1 + \frac{m_2}{m_1}\right)^3 \frac{1}{(2\pi)^3} \int \int d\mathbf{k} d\mathbf{k}' j_0(|\mathbf{k} + \mathbf{k}'|R_1) \frac{1}{|\mathbf{Q}'_2|} \tilde{\phi}_{\ell_h}^*(|\mathbf{Q}'_2|) \frac{1}{|\mathbf{Q}_2|} \tilde{\phi}_{\ell_h}(|\mathbf{Q}_2|) \\ &\quad \times P_{\ell_h}(\cos \widehat{\mathbf{Q}'_2 \mathbf{Q}_2}) \sum_{qJ_q S} (1 + (-1)^{S+q+I_B+1/2-T}) (I_B M_B 1/2 i_h |T M_B + i_h)^2 \hat{J}_q G_{qq}^{J_q ST}(k, k') P_q(\cos \widehat{\mathbf{k} \mathbf{k}'}). \end{aligned} \quad (19)$$

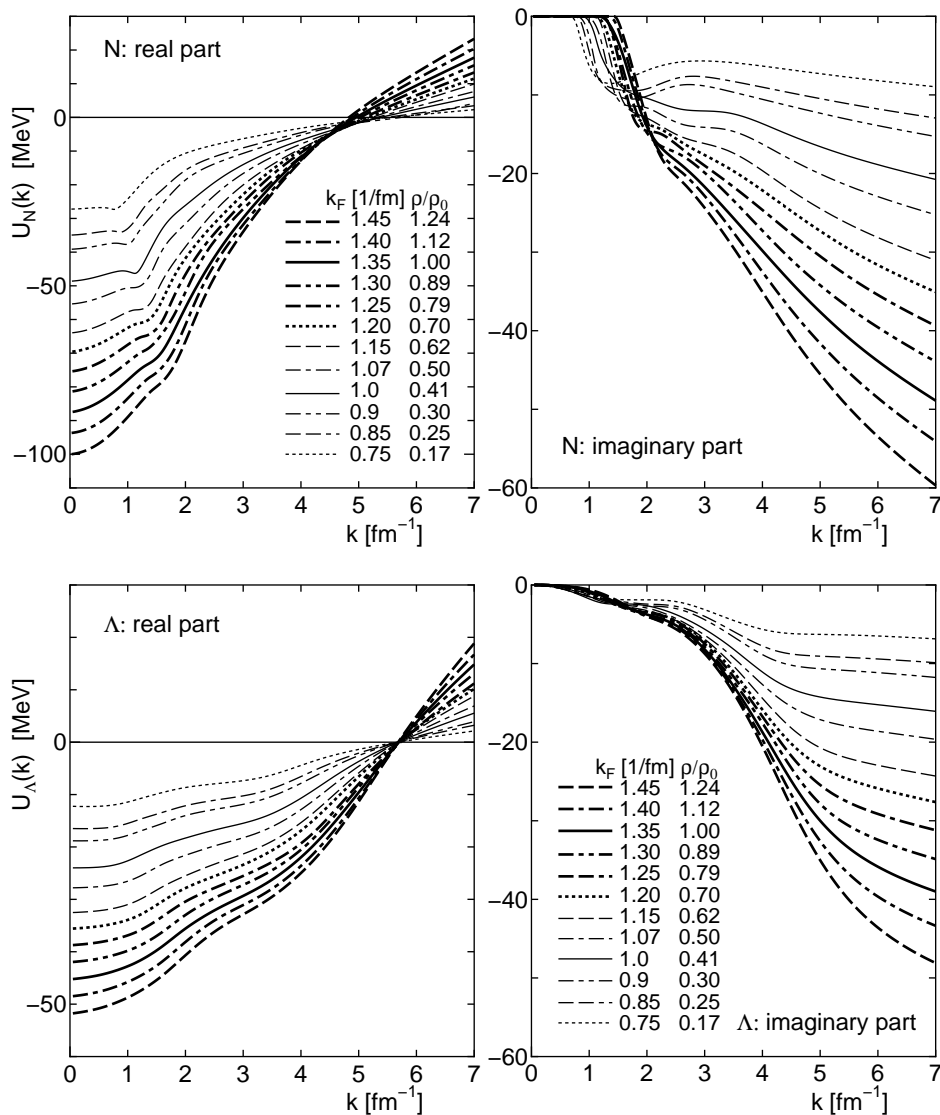


FIG. 1: Real and imaginary parts of single-particle potentials for N and Λ in symmetric nuclear matter at various Fermi momenta, $0.75 \text{ fm}^{-1} \leq k_F \leq 1.45 \text{ fm}^{-1}$.

In the above expression. I_B is the isospin of the baryon for which the s.p. potential is considered, and M_B is its z -component. The index i_h denotes the proton or neutron in the target nucleus.

The Eq. (19) defines a s.p. potential $U_B(R)$ to give

$$I_D + I_E = 4\pi \int R^2 dR |\phi_{\ell j}(R)|^2 U_B(R) \quad (20)$$

It is noted that the potential $U_B(R)$ does not have ℓ - and j -dependences due to approximations introduced in the derivation.

III. SINGLE-PARTICLE POTENTIALS IN SYMMETRIC NUCLEAR MATTER

Before discussing baryon s.p. potentials in finite nuclei, we show s.p. potentials in nuclear matter at various

Fermi momenta, $0.75 \leq k_F \leq 1.45 \text{ fm}^{-1}$, with the quark-model potential fss2 [18]. This potential is defined as a Born kernel of the RGM description of the interaction between the three-quark clusters. We use the energy-independent renormalized version of the fss2 potential [19]. The details of the G -matrix calculation for hyperons in nuclear matter are reported in ref. [20]. It has been known that the LOBT saturation curve in ordinary nuclear matter does not reproduce the empirical saturation property. Although the curve obtained by the potential fss2 with the continuous choice for intermediate spectra almost goes through the empirical saturation point of $k_F = 1.35 \text{ fm}^{-1}$ and $E/A = -16.5 \text{ MeV}$, the energy minimum appears at $k_F = 1.7 \text{ fm}^{-1}$ and $E/A = -20 \text{ MeV}$. Nevertheless the LOBT calculation provides a useful starting point and meaningful information for the baryon s.p. potentials in nuclear medium in the microscopic studies based on the bare baryon-baryon interactions. Missing effects in the LOBT, such as con-

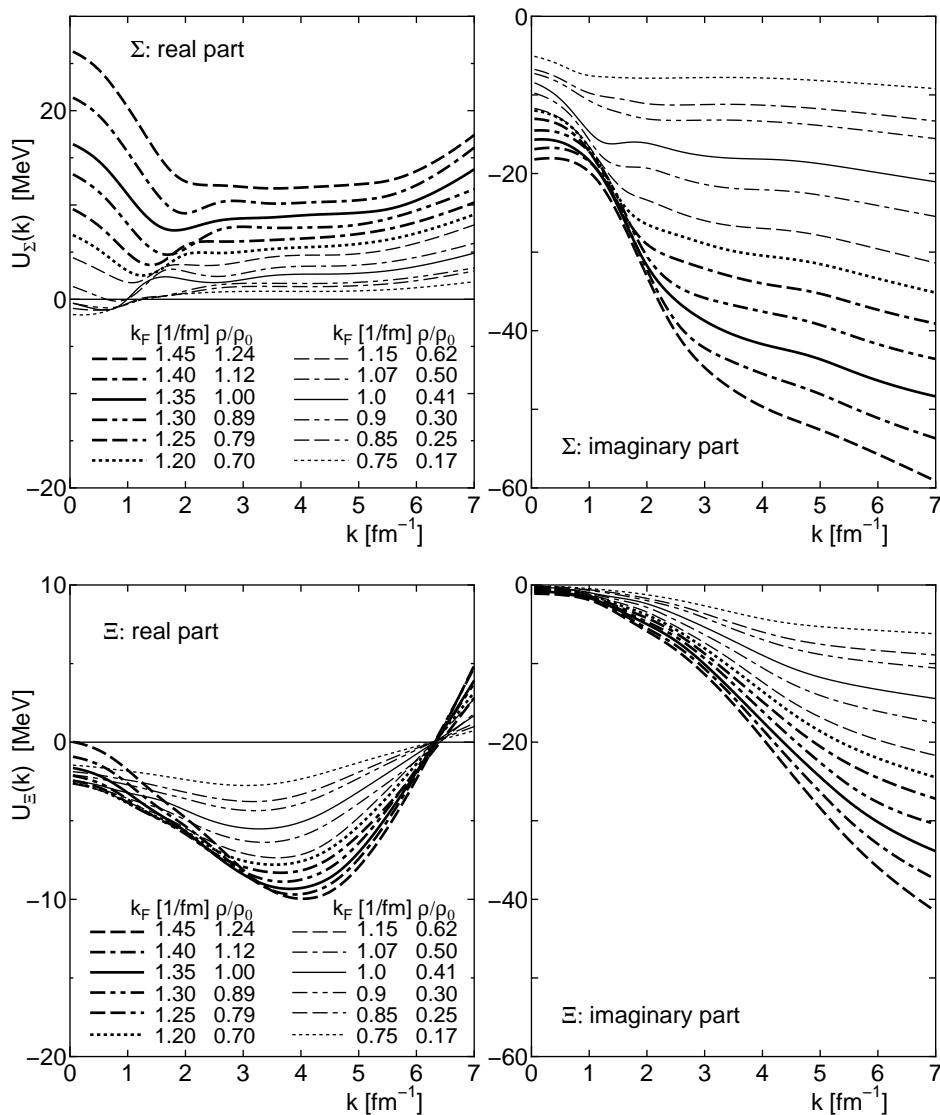


FIG. 2: Real and imaginary parts of single-particle potentials for Σ and Ξ in symmetric nuclear matter at various Fermi momenta, $0.75 \text{ fm}^{-1} \leq k_F \leq 1.45 \text{ fm}^{-1}$.

tributions from higher order diagrams and three-body forces are now semi-quantitatively understood in the nucleon sector [22].

Real and imaginary parts of the calculated s.p. potentials for N , Λ , Σ , and Ξ in symmetric nuclear matter are shown in Figs. 1 and 2 as a function of the momentum k . These are the results after the self-consistency for the starting energy ω being reached. The Fermi momentum k_F is chosen approximately in a step of one tenth of the normal nucleon density ρ_0 . These densities are used as the discretized points of the density in the local density approximation for considering finite nuclei. Below $k_F = 0.75 \text{ fm}^{-1}$, the nuclear matter NN G -matrix calculation becomes unstable due to the appearance of a bound state in the 3S_1 channel. Because we expect little relevance of this phenomenon to ground states of finite nuclei, the instability is not inspected further. In the case that the effective interactions at low density below

$k_F = 0.75 \text{ fm}^{-1}$ is needed in the local density approximation for finite nuclei, we use the G -matrices at $k_F = 0.75 \text{ fm}^{-1}$.

As for the nucleon, the result is very similar to those by other realistic NN potentials. The depth of the s.p. potential at the normal density is considerably larger than the magnitude of the standard Woods-Saxon potential, which is $50 \sim 60 \text{ MeV}$. It has been known that the rearrangement potential reduces the strength by about $10 \sim 20 \text{ MeV}$.

We are concerned mainly with the prediction of the quark-model potential fss2 [18] for hyperon s.p. potentials. The strength of the attractive Λ s.p. potential in normal nuclear matter shown in Fig. 1 is almost 45 MeV , which is again larger than the empirically known value of around 30 MeV . At the low density the potential is shallower. However, as will be shown in the next section, the depth of the calculated Λ s.p. potential in finite

nuclei, taking into account the finite geometry and the effects of the non-diagonal properties of the G , seems to be dictated by the potential depth at the normal nuclear density. We can expect that the rearrangement effects give rise to a repulsive contribution of the order of 10 MeV for the Λ mainly through the energy dependence of the G -matrix.

Nuclear matter calculations using the early version of the Kyoto-Niigata SU_6 quark-model potential, FSS, predicted a repulsive Σ s.p. potential [20]. Results shown in Fig. 2 are obtained by the most recent quark-model parameterization, fss2 [18]. The Σ potential at $k = 0$ is definitely repulsive of about 15 MeV at normal density. This repulsion chiefly comes from the strong repulsive contribution of the 3S_1 state in the isospin $T = \frac{3}{2}$ channel, which is naturally predicted by the quark-model as the consequence of the Pauli principle on the quark level. The interaction in the 1S_0 with $T = \frac{1}{2}$ channel is also repulsive. These repulsive contributions overwhelm the attractive contributions from the 1S_0 with $T = \frac{3}{2}$ and the 3S_1 with $T = \frac{1}{2}$ channels. The width Γ of the Σ hyperon in nuclear medium is related to the imaginary strength of the s.p. potential by $\Gamma(k) = -2\Im U(k)$. $\Gamma(0)$ is seen in Fig. 2 to be more than 30 MeV at normal density.

The Ξ s.p. potential in symmetric nuclear matter predicted by fss2 is weakly attractive as is shown in Fig. 2. As the momentum increases, the magnitude of the attraction is seen to become larger at the low momentum region of $k < 6 \text{ fm}^{-1}$. The momentum dependence may be characterized by the effective mass. To obtain a rough estimation of it, we parameterize the potential by $U_{\Xi}^{\text{real}}(k) \simeq ak^2 + b$. In this case the effective mass at $k = 0$ is obtained by

$$\frac{m_{\Xi}^*}{m_{\Xi}} = \left[1 + \frac{2m_{\Xi}a}{\hbar^2} \right]^{-1} \quad (21)$$

Calculated s.p. potentials give $m_{\Xi}^*/m_{\Xi} \sim 1.1$ at $k_F = 1.35 \text{ fm}^{-1}$ and $m_{\Xi}^*/m_{\Xi} \sim 1.05$ at $k_F = 1.07 \text{ fm}^{-1}$.

The Ξ^-p elastic and inelastic cross-section measurements at low energy by Ahn *et al.* [23] indicate that the width of a Ξ s.p. state in nuclear medium is $\Gamma \sim 3$ MeV. Although it is uncertain at which energy this number should be compared with the calculated imaginary strength, the small imaginary strength of the Ξ s.p. potential at the low momentum region given in Fig. 2 is in accord with the empirical small width of the Ξ in nuclear medium.

It is encouraging to see that the results for Σ and Ξ hyperons agree at least qualitatively with empirical indications so far obtained.

IV. RESULTS IN FINITE NUCLEI

We apply the calculational method presented in Sect. II to from light to medium-heavy nuclei: ^{12}C , ^{16}O , ^{28}Si , ^{40}Ca , ^{56}Fe , and ^{90}Zr . Nucleon density distributions are

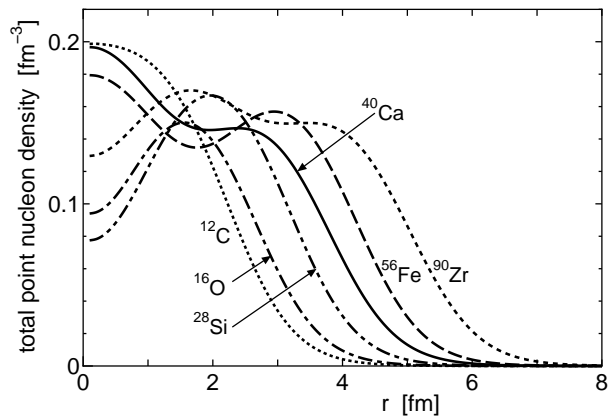


FIG. 3: Point nucleon density distributions $\rho_t(r)$ obtained by DDHF wave functions of the G-0 force [5].

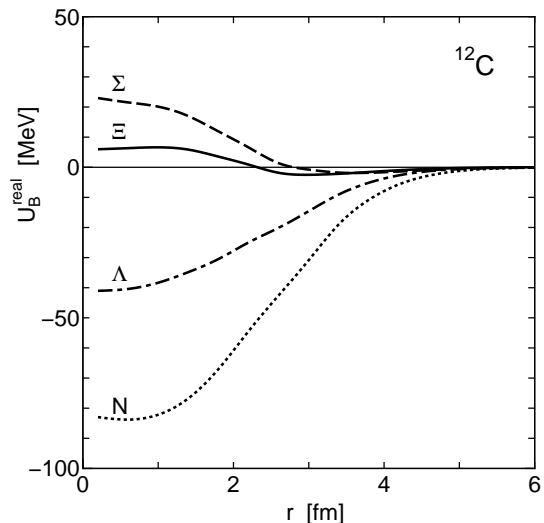
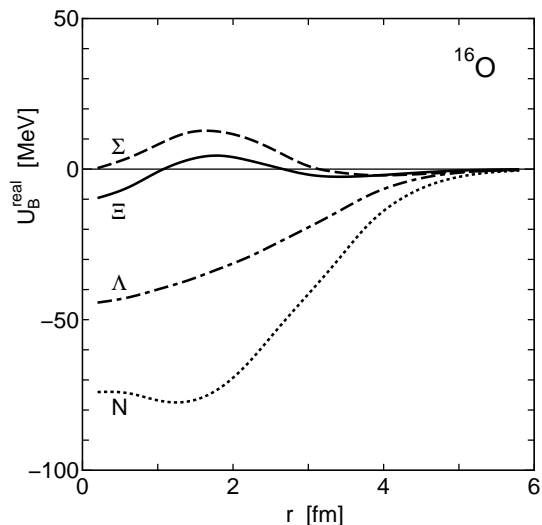
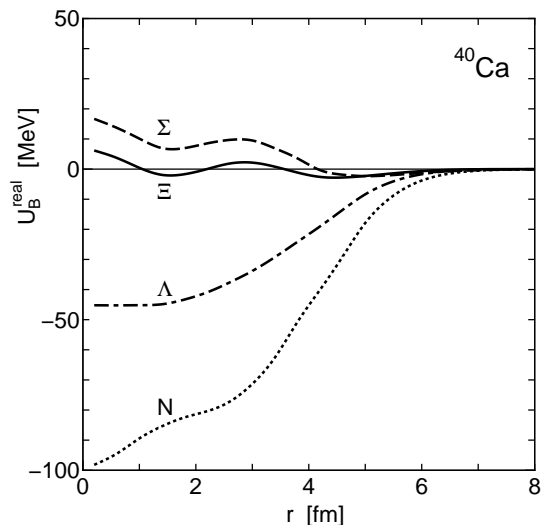
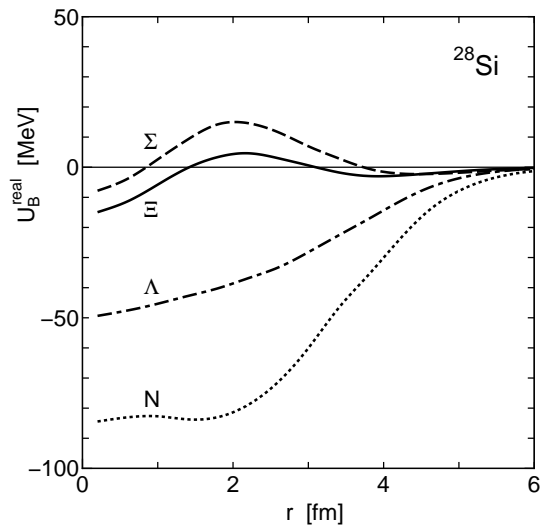
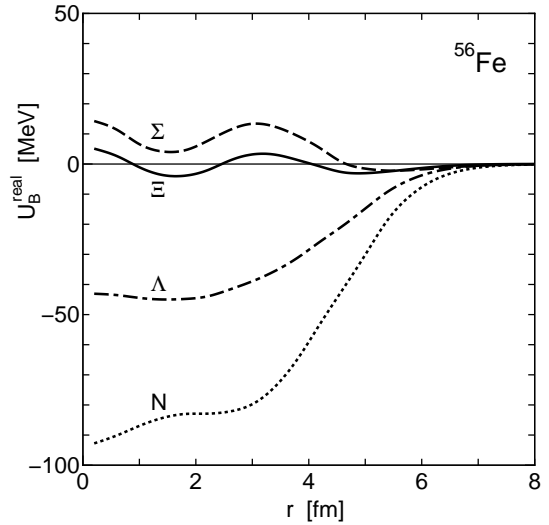


FIG. 4: Real part of localized single-particle potentials for N , Λ , Σ , and Ξ in ^{12}C with the quark-model potential fss2 [18] for the octet baryon-baryon interactions.

prepared by density-dependent Hartree-Fock calculations using the Campi-Sprung G-0 force [5]. Profiles of the point nucleon density distribution $\rho_t(r)$ which is a sum of the neutron and proton densities are shown in Fig. 3.

Nuclear matter G -matrices are used in finite nuclei by the local density approximation. At the position R_1 where the s.p. potential is evaluated the local Fermi momentum is defined by the correspondence $k_F(R_1) = \left[\frac{3\pi^2}{2} \rho_t(R_1) \right]^{1/3}$. The G -matrices calculated in nuclear matter with this Fermi momentum are used in Eq. (19). In actual calculations, G -matrix calculation is carried out only for the Fermi momenta shown in Figs. 1 and 2. At each position R_1 , the Fermi momentum which is closest to $k_F(R_1)$ among these twelve values is cho-

FIG. 5: Same as in Fig. 4, but for ^{16}O .FIG. 7: Same as in Fig. 4, but for ^{40}Ca .FIG. 6: Same as in Fig. 4, but for ^{28}Si .FIG. 8: Same as in Fig. 4, but for ^{56}Fe .

sen. As explained in Sect. II, for small densities below $k_F = 0.75 \text{ fm}^{-1}$, namely the total density $\rho_t = 0.028 \text{ fm}^{-3}$, we always use $k_F = 0.75 \text{ fm}^{-1}$. In homogeneous matter the s.p. potential is determined by the matrix element with the zero momentum transfer, namely diagonal ($\mathbf{k}' = \mathbf{k}$) components of $G(\mathbf{k}', \mathbf{k}; \mathbf{K}, \omega)$. In finite nuclei non-diagonal components of the G matrices also contribute to the s.p. potential.

The starting-energy dependence of the G -matrix plays an important role in the LOBT. The prescription of the starting-energy as the sum of s.p. energies of the two baryons considered means that certain higher-order diagrams are included. Hence the self-consistency between the s.p. energy which is defined by the G -matrix and the G -matrix which depends on the starting-energy is

required. Calculations in nuclear matter shown in Sect. II are the results with this consistency achieved. In the case that the G -matrix in nuclear matter is applied to a finite nucleus, however, there is no simple way to treat the starting-energy dependence. We introduce an ad hoc prescription to use an s.p. potential value at the median momentum $2^{-1/3}k_F$: $\omega = 2m_N + \frac{\hbar^2}{m_N}k^2 + \frac{\hbar^2}{4m_N}K^2 + U_N(2^{-1/3}k_F) + U_N(2^{-1/3}k_F)$ for the nucleon and $\omega = m_Y + m_N + \frac{\hbar^2(m_Y+m_N)}{2m_Y m_N}k^2 + \frac{\hbar^2}{2(m_Y+m_N)}K^2 + U_Y(0) + U_N(2^{-1/3}k_F)$ for the hyperons.

The results with the SU_6 quark-model potential fss2 [18] in the energy-renormalized form are shown in Figs. 4~9. The charge state of the baryon specified by M_B in Eq. (19) is set to be $M_B = -I_B$. Comments on

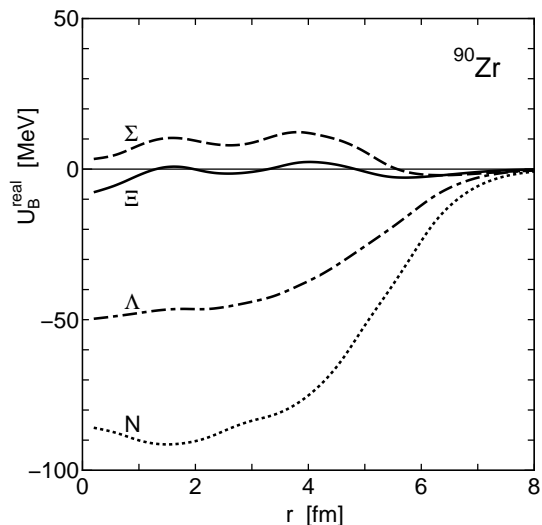


FIG. 9: Same as in Fig. 4, but for ^{90}Zr .

the calculated s.p. potential of each baryon are given in the following.

A. Nucleon s.p. potential

The shape of the calculated nucleon potential is seen to follow the density distribution, and the depth is $80 \sim 90$ MeV which corresponds to the s.p. potential in nuclear matter at the normal density. It is well known that the straightforward application of the LOBT starting from realistic NN interactions overestimate the attractive nucleon-nucleus potential. To compare the calculated potential with the empirical one, we need to include the so-called rearrangement potential. The repulsive strength is known to be $10 \sim 20$ MeV [5]. If this contribution is taken into account, the resulting potential becomes closer to the phenomenological potential of the Woods-Saxon form.

It is noted that it is still a remaining problem in nuclear physics to understand nuclear bulk properties in a fully microscopic way on the basis of the realistic interactions including higher-order correlations, three-body forces, and other possible medium effects.

B. Λ hyperon s.p. potential

The ΛN 1S_0 state has a similar character to the NN 1S_0 state in the spin-flavor SU_6 symmetry, although there is small admixture of a completely quark Pauli forbidden component. Similarly, the interaction in the ΛN 3S_1 channel resembles that in the 3S_1 NN channel with a smaller magnitude by a factor of $1/\sqrt{2}$, although there is an important difference that the pion exchange is absent. Thus it is probable that the Λ -nucleus potential

is attractive, about a half of the N -nucleus potential in magnitude. Looking at the density-dependence of the Λ s.p. potential in nuclear matter, we should expect a similar rearrangement potential as in the nucleon case. The addition of the hyperon to nuclear medium does not change directly the nucleon density and hence the nucleonic Pauli effect. The rearrangement effect for the Λ hyperon originates, in the LOBT, mainly from the energy-dependence of the NN and ΛN G -matrices. If we assume a repulsive rearrangement potential of the order of 10 MeV, calculated results shown in Figs. 4 ~ 9 correspond well to the empirical Λ -nucleus potential in the Woods-Saxon form with the depth of about 30 MeV.

C. Σ hyperon s.p. potential

The experimental information has been limited for the Σ s.p. potential in nuclei. Because the Σ state in a nucleus is expected to have a large width due to the strong $\Sigma N \rightarrow \Lambda N$ conversion process, it is unlikely to observe clear peak structure in the Σ -formation spectra. Nevertheless, results from the early experiments of (K, π) inclusive spectra [24] measured at CERN were interpreted as indicating that the Σ -nucleus potential is moderately attractive. The discovery of the bound $^3\text{He} + \Sigma^0$ and $^3\text{H} + \Sigma^+$ systems [25] and the theoretical consideration by Harada *et al.* [26] showed that the attraction in the ΣN $T = 1/2$ channel should be attractive enough. Another important source of the Σ -nucleus interaction is the energy shift and the width of Σ^- atomic orbits extracted from the X-ray data. Batty, Friedman, and Gal [27] analyzed the data to conclude that the Σ -nucleus potential changes its sign toward higher density region in a nucleus from the attractive potential at the surface region. Dabrowski [28] analyzed the BNL experiment of (K, π) spectrum on ^9Be [29] in a plane wave model and conjectured that the Σ potential is repulsive of the order of 20 MeV. Recent experimental data with better accuracy of (π^-, K^+) inclusive spectra measured at KEK [30] was reported to suggest that the Σ -nucleus potential is strongly repulsive, the strength being more than 100 MeV. Several theoretical analyses carried out later [31, 32] confirmed the repulsive nature of the Σ s.p. potential, but the height may be a few 10 MeV.

On the theoretical side, ΣN interaction models admit large uncertainties. Most parameter sets of the Nijmegen hyperon-nucleon OBEP potential [8, 9, 10, 12] predict an attractive Σ -nucleus potential in nuclear matter, except the model F [33, 34, 35]. On the contrary, the strong repulsive character in the $T = 3/2$ 3S_1 channel is inherent in the quark-model description [18, 36]. Thus the Kyoto-Niigata quark-model potential predicts an overall repulsive Σ s.p. potential in nuclear matter. Results given in Figs. 4~9 show the consequence of this property to finite nuclei. At higher density region inside a nucleus the Σ -nucleus potential is repulsive of $10 \sim 20$ MeV. The overall repulsive nature of the Σ -nucleus potential has

been deduced by the analyses of $(K^-, \pi^+) \Sigma^-$ formation inclusive spectra [30, 31, 32]. Beyond the surface region the potential becomes attractive. It is interesting to see that the radial dependence indicated by the analyses of Σ atomic data [27] is actually derived by the microscopic calculation using the quark-model bare interaction with no phenomenological adjustment.

It is remarked that in the present evaluations we apply G -matrices in symmetric nuclear matter to finite nuclei without separating neutron and proton density distributions. However, in heavy nuclei, e.g. ^{90}Zr in our calculations, in which neutron and proton distributions are visibly different, we should take care of the isospin-dependence when solving the Bethe-Goldstone equation. In that case, the repulsive contribution to the Σ^- s.p. potential from the $T = 3/2$ 3S_1 channel becomes more predominant.

D. Ξ hyperon s.p. potential

For the Ξ s.p. potential, the experimental information has been more scarce than the Σ . The Ξ hyperon is formed in (K^-, K^+) reaction on nuclei with small production rates. There has been no concrete evidence of the Ξ hypernuclear bound state. The existing experimental data of the Ξ formation spectrum [37, 38, 39] has suggested that the Ξ feels attractive potential in nuclei, the depth of which is not so large, $10 \sim 20$ MeV. Our results shown in Figs. 4~9 with the quark-model potential fss2 [18] show that the Ξ -nucleus potential is weakly attractive at and beyond the nuclear surface region, which is similar to the Σ -nucleus potential. Toward the inside of the nucleus the Ξ s.p. potential tends to be repulsive and oscillates around zero with the magnitude of about 10 MeV. It is not possible to simulate the potential shape by a single Woods-Saxon form. No Ξ hypernuclear bound state is expected from such a weak potential. The situation does not change even if the actual potential strength differs by a factor of 2 or so. In that case the level shift of the Ξ^- atomic orbit should be a valuable source of the information about the Ξ -nucleus interaction. This subject is addressed in the next section.

The evaluated ΞN G -matrices include full baryon-channel couplings, namely the possible $\Xi N-\Lambda\Lambda-\Sigma\Sigma$ or $\Xi N-\Lambda\Sigma-\Sigma\Sigma$ couplings. It is helpful to use equivalent interactions in low-momentum space to check the character of the ΞN interaction and the effect of the baryon-channel coupling in each spin and isospin state. Inspecting the matrix elements in ref. [40], we see that the ΞN effective interaction from the fss2 in the $T = 1$ channels both in 1S_0 and 3S_1 are repulsive. The $T = 0$ 3S_1 interaction is very weak, and the $T = 0$ 1S_0 interaction is attractive for which the $\Xi N-\Lambda\Lambda-\Sigma\Sigma$ coupling is responsible. It turns out that the net s -wave contribution is small and thus the attractive p -wave contribution plays an important role to make the Ξ s.p. potential to be attractive at the surface region.

TABLE I: The strength and geometry parameters of the Woods-Saxon form $f_i(r) = U_i^0/[1 + \exp((r - r_{0,i})/a_i)]$ fitted to the real part as well as the imaginary part of Σ and Ξ s.p. potentials $U_B(r)$ in ^{28}Si and ^{56}Fe .

		real part			imaginary part		
		$\sum_{i=1,3} f_i(r)$			$\sum_{i=1,3} f_i(r)$		
^{28}Si	i	U_i^0	$r_{0,i}$	a_i	U_i^0	$r_{0,i}$	a_i
		[MeV]	[fm]	[fm]	[MeV]	[fm]	[fm]
	1	-25.94	4.179	0.7164	-65.63	3.819	0.7539
Σ	2	+57.43	3.049	0.7860	+41.93	3.997	0.8185
	3	-41.13	1.220	0.4348	-6.078	0.3944	1.576
	1	-310.4	2.171	1.066	-6.760	4.980	0.6915
Ξ	2	+543.3	2.959	0.9484	+5.639	5.209	0.6668
	3	-270.3	3.421	0.8630	-1.838	1.118	0.2948
		real part			imaginary part		
		$\sum_{i=1,2} f_i(r) + \frac{df_3(r)}{dr}$			$\sum_{i=1,3} f_i(r)$		
^{56}Fe	i	U_i^0	$r_{0,i}$	a_i	U_i^0	$r_{0,i}$	a_i
		[MeV]	[fm]	[fm]	[MeV]	[fm]	[fm]
	1	-3.746	6.035	0.5655	-65.78	4.955	0.8902
Σ	2	22.19	4.031	0.3990	+37.65	5.486	0.8867
	3	32.22	1.553	0.5527	+16.77	-0.4167	1.163
	1	-2.232	6.367	0.2389	-15.92	5.845	0.6820
Ξ	2	+8.295	3.796	0.2597	+14.64	5.947	0.6728
	3	+20.67	1.674	0.4887	+1.290	0.7581	0.1709

V. ENERGY SHIFT AND WIDTH OF ATOMIC ORBIT

The level shift and the width of Σ^- atomic orbits are a valuable source of the information on the Σ -nucleus strong interaction. The analyses by Batty, Friedman, and Gal [27] indicated that the Σ -nucleus potential is attractive at the surface region, but at higher density region in a nucleus the potential turns to be repulsive. The radial dependence of the calculated Σ^- s.p. potential shown in the previous section agrees with this. Therefore it is instructive to explicitly evaluate the energy shift and the width of Σ^- atomic orbits with the calculated potential. As will be shown below, the result is consistent with the experimental data. This indicates that the microscopic calculation with the quark-model fss2 is reliable in the ΣN channel. Thus, it is interesting to extend the level shift calculation to Ξ^- atomic orbits. The experimental data should be available in near future, because the first measurement of Ξ^- atomic X rays from Fe target is proposed [43] to be performed at J-PARC. The theoretical prediction provides a guiding information for this experiment.

We consider ^{28}Si and ^{56}Fe for explicit evaluations of the level shift of the atomic orbit. We first fit the shape of the calculated s.p. potential using the Woods-Saxon form. For ^{28}Si a sum of three Woods-Saxon shapes is used and for ^{56}Fe a sum of two Woods-Saxon shapes and one

derivative of the Woods-Saxon shape is assigned. Parameters are given in Table I. It is noted that the imaginary parts are also given to illustrate the order of the magnitude of the absorptive strength, intending to demonstrate that the Ξ imaginary potential is about one order of magnitude smaller than the Σ one. However, actual numbers should not be taken very seriously because nuclear matter calculations tend to overestimate the imaginary strength as the calculations [41] of nucleon optical model potential indicates. In addition, the prescription to use the G -matrices at $k_F = 0.75 \text{ fm}^{-1}$ for all the densities below $k_F = 0.75 \text{ fm}^{-1}$ probably leads to the overestimation of the imaginary strength at the surface region. It is also remarked that localized imaginary potential through the zero-momentum Wigner transformation may become positive at some points.

A. Σ^-

Results of the level shift $\Delta E = E - E_C$ and the width $\Gamma = -2\Im E$ for the Σ^- f - and g -atomic levels on ^{28}Si and the Σ^- g - and h -atomic levels on ^{56}Fe are given in Table II, where E_C stands for the Coulomb bound state energy without the Σ^- -nucleus strong interaction. When the real part of the Σ s.p. potential is taken into account, the energy of the $n = 4, \ell = 3$ orbit on ^{28}Si is shifted downward by 222 eV. To investigate the contribution of the absorptive effect, we do not use the calculated potential given in Table I. The imaginary potential is rather strong as explained above. The magnitude of the level shift and the width depends non-linearly on the strength of the imaginary potential. Hence we use an phenomenological imaginary potential to discuss the level shift of the atomic orbits of the Σ^- . We add an imaginary potential in the single Woods-Saxon form used in ref. [27], namely $r_0 = 1.1 \times 28^{1/3}$ and $a = 0.67$ with the depth of -9 MeV. In that case, we obtain $\Delta E = 208$ eV and $\Gamma = 249$ eV, which well correspond to the experimental values of $\Delta E_{exp} = 159 \pm 36$ eV and $\Gamma_{exp} = 220 \pm 110$ eV. This result indicates that the real part of the Σ s.p. potential calculated microscopically in the LOBT starting from the two-body quark-model potential fss2 is reasonable.

B. Ξ^-

Observing that our calculated Σ -nucleus potential gives a reliable result for the shift of the Σ^- atomic level, it is interesting to proceed to Ξ^- atoms without any adjustment. In ref. [42] Batty, Friedman, and Gal estimated the level shift and the width of Ξ^- atoms for the Ξ^- -nucleus potential having an attraction of the depth of 15-20 MeV with an imaginary strength of 1-3 MeV in the shape roughly following a nuclear density distribution. Although the Ξ -nucleus potential is weakly repulsive inside the nucleus in our calculation, the attractive strength at the surface region is found to be comparable to that

TABLE II: The energy shift $\Delta E = E - E_C$ and the width $\Gamma = -2\Im E$ of the Σ^- atomic orbits in ^{28}Si and ^{56}Fe , using the parameterized Σ s.p. potential given in Table I for the real part. The imaginary potential is given in a Woods-Saxon form with the strength $W_0 = -9$ MeV and the geometry parameters $r_0 = 1.1A^{1/3}$ fm and $a = 0.67$ fm. Entry numbers are in eV.

Σ^- - ^{28}Si		
	ΔE_{4f}	Γ_{4f}
real part only	-222	—
real + imaginary	-208	249
exp. [44]	-159 ± 36	220 ± 110
Σ^- - ^{56}Fe		
	ΔE_{5g}	Γ_{5g}
real part only	-0.8	—
real + imaginary	-0.8	0.7
exp. [44]	—	0.41 ± 0.1
Σ^- - ^{56}Fe		
	ΔE_{5g}	Γ_{5g}
real part only	-943	—
real + imaginary	-943	1205
	ΔE_{6h}	Γ_{6h}
real part only	-11	—
real + imaginary	-11	8.3

of the Woods-Saxon potential with the depth of $10 \sim 20$ MeV and the geometry parameters of $r_0 = 1.1A^{1/3}$ fm and $a=0.67$ fm. Results for the f - and g -orbits in ^{28}Si and the g - and h -orbits in ^{56}Fe are given in Table III, together with those of the Woods-Saxon potential as a reference. Because the atomic level shift is insensitive to the short range part of the strong interaction potential, our potential parameterized as shown in Table I, predicts a similar magnitude of the level shift of the reference Woods-Saxon potential. Because the Ξ imaginary potential obtained by the G -matrix is small, we directly use it for the estimation of the width Γ , though it is likely to overestimate the absorptive effect as in the case of Σ^- . As is seen in Table III, the width is of the order of a few hundred eV for the g -orbit in ^{56}Fe and the energy shift is hardly affected. It is needed to see what order of the magnitude is detected for the Ξ^- $n = 5, \ell = 4$ level in ^{56}Fe in the future experiment prepared at J-PARC [43].

VI. SUMMARY

In order to examine the prediction of single-particle properties of all the octet baryons in nuclear medium, especially Ξ hyperon, by the recently developed quark-model baryon-baryon interactions, we have evaluated localized s.p. potentials in finite nuclei by folding G -matrices in nuclear matter with respect to nucleon s.p. wave functions in the scheme of the local density approximation. Introducing a spin-average approximation and a zero-momentum Wigner transformation, the non-local

TABLE III: The energy shift $\Delta E = E - E_C$ and the width $\Gamma = -2\Im E$ of the Ξ^- atomic orbits in ^{28}Si and ^{56}Fe , using the parameterized Ξ s.p. potential given in Table I both for the real and imaginary parts. As a reference, results obtained by the complex Woods-Saxon potential with the strength of $U_0 = -14 - 3i$ MeV, $r_0 = 1.1A^{1/3}$ fm, and $a=0.67$ fm are included. Entry numbers are in eV.

Ξ^- - ^{28}Si		
	ΔE_{4f}	Γ_{4f}
real part only	-346	—
real + imaginary	-345	16
reference pot.	-383	216
Ξ^- - ^{56}Fe		
	ΔE_{5g}	Γ_{5g}
real part only	-6.9	—
real + imaginary	-7.0	0.0
reference pot.	-1.4	0.5
Ξ^- - ^{56}Fe		
	ΔE_{5g}	Γ_{5g}
real part only	-1287	—
real + imaginary	-1281	88
reference pot.	-1675	1092
	ΔE_{6h}	Γ_{6h}
real part only	-12	—
real + imaginary	-12	1.0
reference pot.	-17	8.0

baryon s.p. potential calculated in momentum space is reduced to a local potential in coordinate space. The final expression is feasible for numerical calculations, in the case that the nucleon density distribution is discretized. Adopting about one tenth of the normal nuclear density as the interval of the discretization, we have carried out calculations in ^{12}C , ^{16}O , ^{28}Si , ^{40}Ca , ^{56}Fe , and ^{90}Zr for each octet baryon; N , Λ , Σ , and Ξ . This is the first comprehensive evaluations of the s.p. potentials of all the octet baryons in finite nuclei, starting from the baryon-baryon bare interactions. These microscopic calculations of octet baryon s.p. potentials in finite nuclei are meaningful to elucidate the character of the theoretical model of the octet baryon-baryon interactions by comparing them with empirical s.p. potentials, which are not yet available for the Σ and Ξ hyperons.

We use the most recent quark-model potential, fss2 [18] as bare baryon-baryon interactions. The energy-dependence in the original form of the quark-model potential is eliminated by the renormalization procedure. The NN sector of this potential describes scattering data as accurately as other modern realistic interaction. Calculated nucleon s.p. potentials in nuclear medium are found to be similar to those obtained in the LOBT framework with other potentials. The ΛN interaction is under control to a certain extent by the experimental data of Λ hypernuclei. The fss2 gives similar Λ s.p. potentials in nuclear medium to those of the Nijmegen OBEP po-

tential. It was shown [40] in fact that the fss2 and the Nijmegen NSC97f actually have very similar matrix elements of the equivalent interaction in low-momentum space.

The extension to the ΣN channel and further to the ΞN sector of the strangeness $S = -2$ has many ambiguities because of scarcity of experimental information. It is necessary to rely on the theoretical framework as reliable as possible to construct these baryon-baryon interactions. At present, the SU_6 quark-model fss2 is more predictive than the OBEP model, in the sense that the potential parameters are uniquely given in contrast to various sets of parameters presented by the Nijmegen group. Thus we focus our attention in this paper on the fss2 as the input ΣN and ΞN two-body interactions. The comparison with the results by other potential models including the parameterization based on the effective chiral field approach [45, 46] is an interesting future subject.

Properties of the calculated Σ s.p. potential in finite nuclei are found to agree well with the experimental evidence so far obtained. The potential is repulsive of the order of 10-20 MeV, which is necessary to accounts for the $(\pi^-, K^+) \Sigma^-$ formation spectra on nuclei [31, 32], while it should be attractive at the surface region, as the atomic level shifts indicate [27]. The attraction obtained by the present microscopic calculation can reproduce the empirical energy shifts of the Σ^- atomic levels. To determine more precisely the shape and the strength of the Σ -nucleus potential including its isospin-dependence and study the relation to the underlying bare interaction, we need further experimental data.

On the basis of these observations, it is interesting to consider the ΞN sector. The imaginary part of the Ξ s.p. potential is small in the quark model description, which is consistent with the empirical estimation based on the $\Xi^- p$ scattering cross-section at low energy [23]. Therefore, if the real part is sufficiently attractive to sustain hypernuclear bound states, we can expect clear spike structure in the (K^-, K^+) inclusive spectra on nuclei. At the surface region the potential has similar attraction to the Σ potential. However, the potential does not have a familiar shape simulated well by a Woods-Saxon form. Inside the nucleus the potential fluctuates around zero, reflecting the fluctuation of the nucleon density distribution. The quark model potential fss2 implies that the net s -wave contribution to the Ξ s.p. potential is small and the net weakly attractive contribution from the p -waves is relatively important. Such a potential does not support Ξ nuclear bound states. In that case, measurements of the energy shift and width of the Ξ atomic level become an invaluable source of the information about the Ξ -nucleus strong interaction. Our Ξ s.p. potential calculated by the fss2 suggests that the negative energy shift is the order of a few hundred eV for the $4f$ -orbit in ^{28}Si and the order of 1 keV for $5g$ -orbit in ^{56}Fe . The existence or non-existence of Ξ hypernuclear bound states and the energy shifts of the Ξ^- atomic states will be clarified in near future by the experiments prepared in the J-PARC

project [47], which should advance our understanding of the interactions in the $S = -2$ sector. Our calculational framework provide a useful method to link the baryon s.p. properties in nuclei with the two-body interactions between octet baryons.

Acknowledgments

This study was supported by Grant-in-Aids for Scientific Research (C) from the Japan Society for the Promotion of Science (Grants nos. 17540263 and 18540261).

-
- [1] K.A. Brueckner, C.A. Levinson, and H.M. Mahmoud, Phys. Rev. **95**, 217 (1954).
 [2] K.A. Brueckner and C.A. Levinson, Phys. Rev. **97**, 1344 (1955).
 [3] B.D. Day, Rev. Mod. Phys. **39**, 719 (1967).
 [4] J.W. Negele, Phys. Rev. **C1**, 1260 (1970).
 [5] X. Campi and D.W.L. Sprung, Nucl. Phys. **A194**, 401 (1972).
 [6] O. Hashimoto and H. Tamura, Prog. Part. Nucl. Phys. **57**, 564 (2006).
 [7] H. Horiuchi, Prog. Theor. Phys. **64**, 830 (1980).
 [8] M.M. Nagels, Th.A. Rijken, and J.J. de Swart, Phys. Rev. **D15**, 2547 (1977).
 [9] M.M. Nagels, Th.A. Rijken, and J.J. de Swart, Phys. Rev. **D20**, 1633 (1979).
 [10] P.M.M. Maessen, Th.A. Rijken, and J.J. de Swart, Phys. Rev. **C40**, 2226 (1989).
 [11] Th.A. Rijken, V.G.J. Stoks, and Y. Yamamoto, Phys. Rev. **C59**, 21 (1999).
 [12] V.G.J. Stoks and Th.A. Rijken, Phys. Rev. **C59**, 3009 (1999).
 [13] Th.A. Rijken and Y. Yamamoto, Phys. Rev. **C73**, 044008 (2006).
 [14] Y. Fujiwara, C. Nakamoto, and Y. Suzuki, Prog. Theor. Phys. **94**, 215 and 353 (1995).
 [15] Y. Fujiwara, C. Nakamoto, and Y. Suzuki, Phys. Rev. Lett. **76**, 2242 (1996).
 [16] Y. Fujiwara, C. Nakamoto, and Y. Suzuki, Phys. Rev. **C54**, 2180 (1996).
 [17] Y. Fujiwara, M. Kohno, C. Nakamoto, and Y. Suzuki, Phys. Rev. **C64**, 054001 (2001).
 [18] Y. Fujiwara, Y. Suzuki, and C. Nakamoto, Prog. Part. Nucl. Phys. **58**, 439 (2007).
 [19] Y. Suzuki, H. Matsumura, M. Orabi, Y. Fujiwara, P. Descouvemont, M. Theeten, and D. Baye, Phys. Lett. **B659**, 160 (2008).
 [20] M. Kohno, Y. Fujiwara, T. Fujita, C. Nakamoto, and Y. Suzuki, Nucl. Phys. **A674**, 229 (2000).
 [21] Y. Fujiwara and M. Kohno, in preparation.
 [22] M. Baldo, Lecture Notes in Physics **578**, 1 (2001).
 [23] J.K. Ahn *et al.*, Phys. Lett. **B633**, 214 (2006).
 [24] R. Bertini *et al.*, Phys. Lett. **B90**, 375 (1980); **B136**, 29 (1984); **B158**, 19 (1985).
 [25] T. Nagae *et al.*, Phys. Rev. Lett. **80**, 1605 (1998).
 [26] T. Harada, Phys. Rev. Lett. **81**, 5287 (1998).
 [27] C.J. Batty, E. Friedman, and A. Gal, Phys. Lett. **B335** (1994) 273; Phys. Rep. **287**, 385 (1997).
 [28] J. Dabrowski, Phys. Rev. **C60**, 025205 (1999).
 [29] R. Sawafta, Nucl. Phys. **A585**, 103c (1995); **A639**, 103c (1998).
 [30] H. Noumi *et al.*, Phys. Rev. Lett. **89**, 072301 (2002).
 [31] T. Harada and Y. Hirabayashi, Nucl. Phys. **A759**, 143 (2005).
 [32] M. Kohno, Y. Fujiwara, Y. Watanabe, K. Ogata, and M. Kawai, Phys. Rev. **C74**, 064613 (2006).
 [33] Y. Yamamoto and H. Bando, Prog. Theor. Phys. **73**, 905 (1985).
 [34] Y. Yamamoto and H. Bando, Prog. Theor. Phys. **83**, 254 (1990).
 [35] H.-J. Schulze, M. Baldo, U. Lombardo, J. Cugnon, and A. Lejeune, Phys. Rev. **C57**, 704 (1998).
 [36] M. Oka, K. Shimizu, and K. Yazaki, Prog. Theor. Phys. Suppl. **137**, 1 (2000).
 [37] T. Iijima *et al.*, Nucl. Phys. **A546**, 588 (1992).
 [38] T. Fukuda *et al.*, Phys. Rev. **C58**, 1306 (1998).
 [39] P. Khaustov *et al.*, Phys. Rev. **C61**, 054603 (2000).
 [40] M. Kohno, R. Okamoto, H. Kamada, and Y. Fujiwara, Phys. Rev. **C76**, 064002 (2007).
 [41] N. Yamaguchi, S. Nagata, and T. Matsuda, Prog. Theor. Phys. **70**, 459 (1987).
 [42] C.J. Batty, E. Friedman, and A. Gal, Phys. Rev. **C59**, 295 (1999).
 [43] K. Tanida *et al.*, proposal E03 for J-PARC 50 GeV Proton Synchrotron (2006).
 [44] C.J. Batty *et al.*, Phys. Lett. **B74**, 27 (1978).
 [45] H. Polinder, J. Haidenbauer, and U.-G. Meißner, Nucl. Phys. **A779**, 244 (2006).
 [46] H. Polinder, J. Haidenbauer, and U.-G. Meißner, Phys. Lett. **B653**, 29 (2007).
 [47] T. Nagae, Nucl. Phys. **A805**, 486c (2008).